Reduction of the K^* meson abundance in heavy ion collisions

Sungtae Cho[1] and Su Houng Lee[2]
[1]Division of Science Education, Kangwon National University, Chuncheon 24341, Korea
[2]Department of Physics and Institute of Physics and Applied Physics, Yonsei University, Seoul 03722, Korea

(Received 18 October 2015; revised manuscript received 26 January 2018; published 12 March 2018)

We study the K^* meson reduction in heavy-ion collisions by focusing on the hadronic effects on the K^* meson abundance. We evaluate the absorption cross sections of the K^* and K meson by light mesons in the hadronic matter, and further investigate the variation in the meson abundances for both particles during the hadronic stage of heavy-ion collisions. We show how the interplay between the interaction of the K^* meson and kaon with light mesons in the hadronic medium determines the final yield difference of the statistical hadronization model to the experimental measurements. For the central Au+Au collision at $\sqrt{s_{NN}} = 200$ GeV, we find that the K^*/K yield ratio at chemical freeze-out decreases by 37% during the expansion of the hadronic matter, resulting in the final ratio comparable to STAR measurements of 0.23 $\pm$0.05.

DOI: 10.1103/PhysRevC.97.034908

I. INTRODUCTION

Relativistic heavy-ion collision experiments have enabled the production of a system of quantum chromodynamic matter at extreme conditions under controlled conditions [1–5]. Due to the huge energies available in heavy-ion collisions, it is expected that a possible phase transition predicted by Lattice Quantum Chromodynamics [6] between a hadronic matter and a system of deconfined quarks and gluons takes place, and the quark-gluon plasma at very high temperature is produced at the initial stage of the collision. As a result, large numbers of hadronic particles are produced during the quark-hadron phase transition at later stages of heavy-ion collisions.

These hadronic particles are believed to emerge at the transition point with the information of the matter. The statistical hadronization model has been quite successful in explaining the measured production yields of hadrons with two parameters characterizing the chemical freeze-out point in heavy-ion collisions: the phase transition temperature and the baryon chemical potential [7–10].

All particles produced at the freeze-out, however, are subject to further interactions with other hadrons in the hadronic matter, leading to possible deviations in the final yield of some hadrons from the statistical model prediction. In addition to the effects from hadronic interactions, the lifetime of hadrons as well as the lifetime of the hadronic matter itself plays an important role in changing the abundance of hadrons from the yield at the chemical freeze-out.

The abundance of hadrons that are stable against strong decays is expected to be changed mostly by hadronic interactions while that of resonances will be affected by both their interactions with other hadrons and their strong decays when the lifetime of resonances is comparable to or smaller than the lifespan of the hadronic stage in heavy-ion collisions. Daughter particles of resonances are subject to rescatter as well in the hadronic medium, making the reconstruction of the resonances from an invariant mass analysis difficult.

Studying the effects from the hadronic interactions on the abundance of resonances has been suggested as one way of confirming the scenario about a time delay between the chemical and thermal freeze-out [11,12], since a sudden hadronization in heavy-ion collisions would leave no time for resonances to decay in the hadronic medium. In particular, the K^* meson has attracted lots of attention as its short lifetime 4 fm/c is less than the presumed lifespan of the hadronic stage.

The effects of hadronic interactions on the yield of the K^* meson have been measured in heavy-ion collisions using K^*/K yield ratios. Since the K meson is the ground state of the K^* meson, having the same valence quarks with a different mass and relative orientation of its quark spins, the K^*/K yield ratio is considered to be independent of the freeze-out conditions when hadronic interactions are neglected. It has been shown that K^*/K yield ratios decrease with the increasing size of the system at the same energy [13,14]. Compared to p+p collisions, K^*/K yield ratios in Cu+Cu and Au+Au collisions are smaller, naively implying that K^* and K mesons participate in rescattering processes during the expansion of hadronic matter, and that the hadronic effects become larger as the size of the hadronic matter increases.

The average transverse momentum of the K^* meson measured in heavy-ion collisions [13,14], which is higher than that of the K^* meson in p+p collisions, also supports the rescattering scenario about K^* mesons. K^* mesons with low transverse momenta escape the hadronic stage later than K^* mesons with higher transverse momenta, and thus suffer more rescattering in the hadronic medium. As a result the measurement of the K^*/K yield ratio 0.23 ± 0.05 [13] in Au+Au collision at $\sqrt{s_{NN}} = 200$ GeV is smaller than the statistical model expectation 0.33 ± 0.01 at that collision [10]. However, as we will see, the measurement of the K^*/K yield ratio that is inconsistent with the statistical model prediction not only confirms the hadronic effects on the yield of the K^* meson but also provides information on the change in the properties of the hadronic matter at freeze-out.

The hadronic effects on the abundance of the K^* meson in the hadronic matter have been studied in many literatures [11,12,15–20]. A microscopic transport approach to hadronic interactions, the UrQMD model [21,22], has been successful in explaining experimental measurements of the K^* meson in heavy-ion collisions, e.g., the transverse momentum distributions of K^* mesons in different centralities and the ratio of yield K^{*0}/K^- [20] recently measured at CERN's Large Hadron Collider (LHC) [23].

There also have been attempts to understand the abundance of K^* mesons at chemical freeze-out by investigating the relative abundance between daughter particles of the K^* meson, $\langle K/\pi\rangle$ [15,16]. Based on the analysis of the fluctuation between same charged particles, K^- and π^-, and opposite charged particles, K^+ and π^-, the constraint on the K^* meson reinteraction between chemical and thermal freeze-out has been studied [19].

With these investigations of the K^*/K yield ratio in mind, we study here the hadronic effects on the K^* meson by evaluating its absorption cross sections with π,ρ,K, and K^* mesons, and furthermore investigate variations in the K^* meson abundance during the hadronic stage of heavy-ion collisions by solving a time evolution equation for the K^* meson. After the K^* meson is produced at the chemical freeze-out, it interacts mostly with light hadrons during the expansion of the hadronic matter. As a result, K^* mesons can be absorbed by the comoving light mesons, or additionally produced from scattering between them. Thus, evaluating the K^* meson cross sections by light hadrons is necessary in estimating the hadronic effects on the K^* meson abundance in heavy-ion collisions. By comparing our results with the experimental observation in heavy-ion collisions, we understand the discrepancy of the K^* meson yield between the statistical model and the experimental measurements.

As has been stated, the scattering of the K^* meson daughter particles such as kaons in the hadronic medium also contains useful information in understanding the hadronic effects on K^* mesons. Therefore, we also take into account interactions of the kaon with light mesons during the hadronic stage of heavy-ion collisions.

To this end, we introduce effective Lagrangians for interactions between light mesons. The effective Lagrangian methods have been used to calculate the scattering cross sections between J/ψ and hadrons in order to estimate the amount of J/ψ suppression in the hadronic matter [24–27]. Similar approaches have been applied to investigate the hadronic effects on the abundance of ϕ mesons [28], and exotic mesons such as $D_{sJ}(2317)$ [29] and $X(3872)$ mesons [30,31].

This paper is organized as follows. In Sec. II, we first consider interactions of both the K^* meson and kaon with light mesons. Then we evaluate the absorption cross sections of both mesons in the hadronic medium using effective Lagrangians. In Sec. III we investigate the time evolution of the K^* meson abundance by solving the kinetic equation. In Sec. IV, we argue the important roles of the abundance ratio of K^* mesons to kaons in heavy-ion collisions. Section IV is devoted to conclusions. We discuss in detail the contact term in the Appendix.

We have used throughout the paper the isospin averaged mass for all hadrons, based on experimentally measured masses [32], e.g., $m_K = 495.645$ MeV.

II. HADRONIC EFFECTS ON K^* AND K MESONS

We first investigate hadronic interactions of a K^* meson during the hadronic stage of heavy-ion collisions. The K^* meson produced at the chemical freeze-out can be absorbed or even produced through interactions between mostly light mesons during the expansion of the hadronic matter. We consider here the K^* meson interacting with pions, ρ mesons, kaons, and K^* mesons; $K^*\pi\to\rho K$, $K^*\rho\to\pi K$, $K^*\bar{K}\to\rho\pi$, $K^*\bar{K}^*\to\pi\pi$, and $K^*\bar{K}^*\to\rho\rho$. The diagrams representing each process are shown in Fig. 1. We introduce the following Lagrangians to describe the interaction between the K^* meson and other mesons:

$$\begin{aligned}
\mathcal{L}_{\pi KK^*} &= ig_{\pi K^*K}K^{*\mu}\vec{\tau}\cdot(\bar{K}\partial_\mu\vec{\pi}-\partial_\mu\bar{K}\vec{\pi})+\text{H.c.},\\
\mathcal{L}_{\rho KK} &= ig_{\rho KK}(K\vec{\tau}\partial_\mu\bar{K}-\partial_\mu K\vec{\tau}\bar{K})\cdot\vec{\rho}^{\mu},\\
\mathcal{L}_{\rho K^*K^*} &= ig_{\rho K^*K^*}[(\partial_\mu K^{*\nu}\vec{\tau}\bar{K}^*_\nu-K^{*\nu}\vec{\tau}\partial_\mu\bar{K}^*_\nu)\cdot\vec{\rho}^{\mu}\\
&\quad+(K^{*\nu}\vec{\tau}\cdot\partial_\mu\vec{\rho}_\nu-\partial_\mu K^{*\nu}\vec{\tau}\cdot\vec{\rho}_\nu)\bar{K}^{*\mu}\\
&\quad+K^{*\mu}(\vec{\tau}\cdot\vec{\rho}^{\nu}\partial_\mu\bar{K}^*_\nu-\vec{\tau}\cdot\partial_\mu\vec{\rho}^{\nu}\bar{K}^*_\nu)],\\
\mathcal{L}_{\pi\rho KK^*} &= -g_{\pi\rho KK^*}K^{*\mu}(2\vec{\tau}\cdot\vec{\pi}\vec{\tau}\cdot\vec{\rho}_\mu-\vec{\tau}\cdot\vec{\rho}_\mu\vec{\tau}\cdot\vec{\pi})\bar{K}\\
&\quad+\text{H.c.}, \qquad (1)\\
\mathcal{L}_{\pi\pi K^*K^*} &= g_{\pi\pi K^*K^*}\left(\frac{\vec{\pi}\cdot\vec{\pi}}{2}\right)K^{*\mu}\bar{K}^*_\mu,\\
\mathcal{L}_{\rho\rho KK} &= g_{\rho\rho KK}\left(\frac{\vec{\rho}^{\mu}\cdot\vec{\rho}_\mu}{2}\right)K\bar{K},\\
\mathcal{L}_{\rho\rho K^*K^*} &= g_{\rho\rho K^*K^*}K^{*\mu}(2\vec{\tau}\cdot\vec{\rho}_\nu\vec{\tau}\cdot\vec{\rho}_\mu-\vec{\tau}\cdot\vec{\rho}_\mu\vec{\tau}\cdot\vec{\rho}_\nu\\
&\quad-\vec{\rho}^{\sigma}\cdot\vec{\rho}_\sigma g_{\mu\nu})\bar{K}^{*\nu},
\end{aligned}$$

obtained from free pseudoscalar and vector meson Lagrangians by introducing the minimal substitution. In Eq. (1), $K\equiv(K^0,K^+)$ and $K^*\equiv(K^{*0},K^{*+})$ denote strangeness pseudoscalar and vector meson doublets, respectively, and $\vec{\pi}$ and $\vec{\rho}$ denote the pion and ρ meson isospin triplets, respectively, with Pauli matrices $\vec{\tau}$. $g_{\pi K^*K}$, $g_{\rho KK}$, and $g_{\rho K^*K^*}$ are strong-coupling constants, for which we use the empirical values $g_{\pi K^*K}=3.25$ and $g_{\rho KK}=3.05$ [33]. We apply the SU(3) flavor symmetry to obtain $g_{\rho K^*K^*}=g_{\pi K^*K}=3.25$, $g_{\pi\rho KK^*}=g_{\pi K^*K}g_{\rho KK}$, $g_{\pi\pi K^*K^*}=2g^2_{\pi K^*K}$, $g_{\rho\rho KK}=2g^2_{\rho KK}$, and $g_{\rho\rho K^*K^*}=g^2_{\rho K^*K^*}$.

Here we neglect the $KK\pi\pi$ contact term since its contribution is smaller than that from the vector meson mediated pseudoscalar four point contact term as explained in the Appendix. In addition to the interactions shown in Eq. (1), one may consider anomalous interactions [27,34]. Recently, the importance of the anomalous contribution to the dissociation and recombination of vector mesons in the hadron medium have been discussed [35,36].

The work with the anomalous contributions will involve a careful discussion of the couplings in connection to the anomalous contributions coming from the gauged Wess-Zumino action in the so-called Bardeen form in SU(3). This

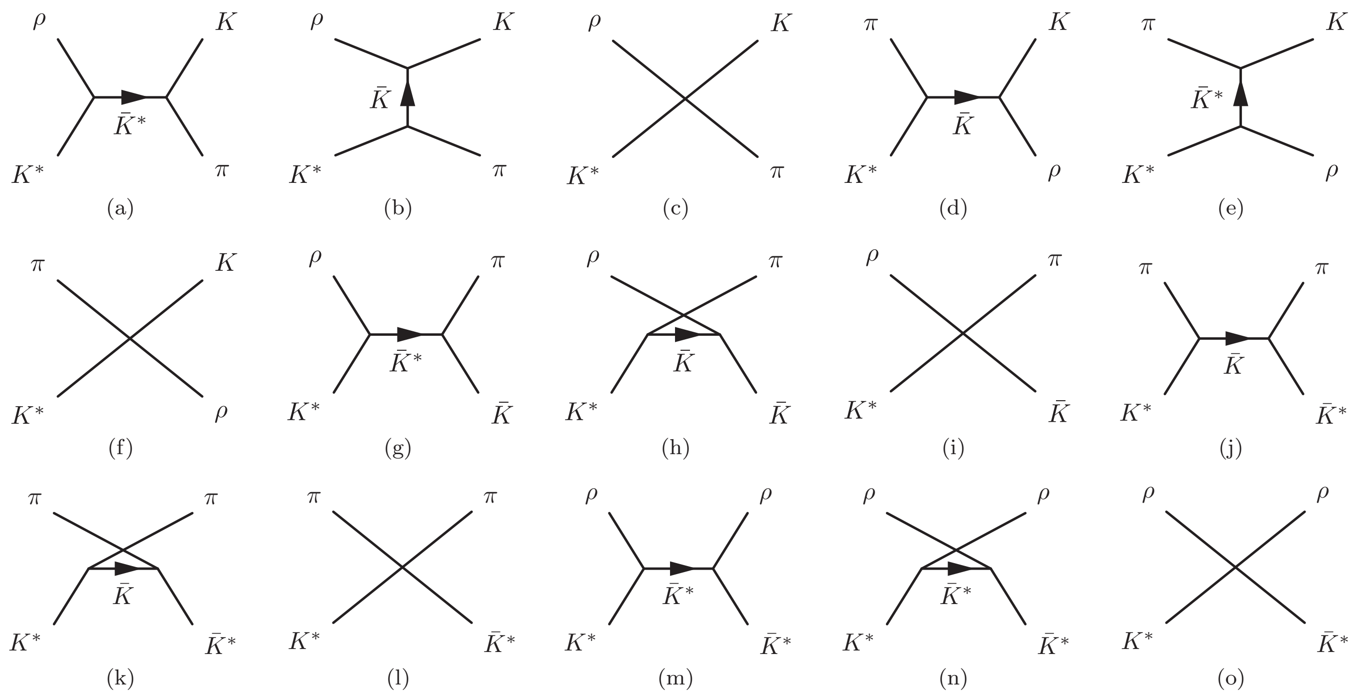

FIG. 1. Born diagrams for the K^* meson absorption by π, ρ, K, and K^* mesons. (a–c) $K^*\pi \to \rho K$. (d–f) $K^*\rho \to \pi K$. (g–i) $K^*\bar{K} \to \rho\pi$. (j–l) $K^*\bar{K}^* \to \pi\pi$. (m–o) $K^*\bar{K}^* \to \rho\rho$.

is an important subject that deserves a separate discussion, and therefore we restrict in the present paper our discussion to contributions available from the interaction Lagrangians, Eq. (1), and investigate the anomalous contributions in future work.

Using the above interaction Lagrangians we evaluate the amplitudes for all processes shown in Fig. 1. The amplitudes of the K^* meson absorption by π, ρ, K, and K^* mesons, without isospin factors and before summing and averaging over external spins, are represented by

$$\mathcal{M}_{K^*\pi\to\rho K} \equiv \mathcal{M}_{K^*}^{(a)} + \mathcal{M}_{K^*}^{(b)} + \mathcal{M}_{K^*}^{(c)}, \quad \mathcal{M}_{K^*\rho\to\pi K} \equiv \mathcal{M}_{K^*}^{(d)} + \mathcal{M}_{K^*}^{(e)} + \mathcal{M}_{K^*}^{(f)}, \quad \mathcal{M}_{K^*\bar{K}\to\rho\pi} \equiv \mathcal{M}_{K^*}^{(g)} + \mathcal{M}_{K^*}^{(h)} + \mathcal{M}_{K^*}^{(i)},$$
$$\mathcal{M}_{K^*\bar{K}^*\to\pi\pi} \equiv \mathcal{M}_{K^*}^{(j)} + \mathcal{M}_{K^*}^{(k)} + \mathcal{M}_{K^*}^{(l)}, \quad \mathcal{M}_{K^*\bar{K}^*\to\rho\rho} \equiv \mathcal{M}_{K^*}^{(m)} + \mathcal{M}_{K^*}^{(n)} + \mathcal{M}_{K^*}^{(o)}, \tag{2}$$

where the amplitudes for the first $K^*\pi \to \rho K$ and the second process $K^*\rho \to \pi K$ are

$$\mathcal{M}_{K^*}^{(a)} = g_{\pi K^* K} g_{\rho K^* K^*} \epsilon_1^{\alpha} \epsilon_3^{*\beta} \frac{1}{t - m_{K^*}^2 + i m_{K^*}\Gamma_{K^*}} \left[-g^{\mu\nu} + \frac{(p_1 - p_3)^{\mu}(p_1 - p_3)^{\nu}}{m_{K^*}^2}\right](p_2 + p_4)_{\mu}$$
$$\times [(2p_1 - p_3)_{\beta} g_{\alpha\nu} - (p_1 + p_3)_{\nu} g_{\alpha\beta} - (p_1 - 2p_3)_{\alpha} g_{\beta\nu}],$$
$$\mathcal{M}_{K^*}^{(b)} = -g_{\pi K^* K} g_{\rho K K} \epsilon_1^{\alpha} \epsilon_3^{*\beta} \frac{1}{s - m_K^2} (p_1 + 2p_2)_{\alpha} (p_3 + 2p_4)_{\beta}, \quad \mathcal{M}_{K^*}^{(c)} = -g_{\pi\rho K K^*} \epsilon_1^{\alpha} \epsilon_3^{*\beta} g_{\alpha\beta} \tag{3}$$

and

$$\mathcal{M}_{K^*}^{(d)} = -g_{\pi K^* K} g_{\rho K K} \epsilon_1^{\alpha} \epsilon_2^{\beta} \frac{1}{t - m_K^2} (p_1 - 2p_3)_{\alpha} (2p_4 - p_2)_{\beta},$$
$$\mathcal{M}_{K^*}^{(e)} = -g_{\pi K^* K} g_{\rho K^* K^*} \epsilon_1^{\alpha} \epsilon_2^{\beta} \frac{1}{s - m_{K^*}^2 + i m_{K^*}\Gamma_{K^*}} \left[-g^{\mu\nu} + \frac{(p_1 + p_2)^{\mu}(p_1 + p_2)^{\nu}}{m_{K^*}^2}\right](p_3 - p_4)_{\mu}$$
$$\times [(2p_1 + p_2)_{\beta} g_{\alpha\nu} - (p_1 - p_2)_{\nu} g_{\alpha\beta} - (p_1 + 2p_2)_{\alpha} g_{\beta\nu}],$$
$$\mathcal{M}_{K^*}^{(f)} = -g_{\pi\rho K K^*} \epsilon_1^{\alpha} \epsilon_2^{\beta} g_{\alpha\beta}, \tag{4}$$

respectively. Similarly, amplitudes for processes $K^*\bar{K} \to \rho\pi$ and $K^*\bar{K}^* \to \pi\pi$ are

$$\mathcal{M}_{K^*}^{(g)} = g_{\pi K^* K} g_{\rho K^* K^*} \epsilon_1^{\alpha} \epsilon_3^{*\beta} \frac{1}{t - m_{K^*}^2 + i m_{K^*}\Gamma_{K^*}} \left[-g^{\mu\nu} + \frac{(p_1 - p_3)^{\mu}(p_1 - p_3)^{\nu}}{m_{K^*}^2}\right](p_2 + p_4)_{\mu}$$
$$\times [(2p_3 - p_1)_{\alpha} g_{\beta\nu} - (p_1 + p_3)_{\nu} g_{\alpha\beta} + (2p_1 - p_3)_{\beta} g_{\alpha\nu}],$$

$$\mathcal{M}^{(h)}_{K^*} = g_{\pi K^* K} g_{\rho K K} \epsilon_1^{\alpha} \epsilon_3^{*\beta} \frac{1}{u - m_K^2} (2p_4 - p_1)_{\alpha} (2p_2 - p_3)_{\beta},$$
$$\mathcal{M}^{(i)}_{K^*} = -g_{\pi\rho K K^*} \epsilon_1^{\alpha} \epsilon_3^{*\beta} g_{\alpha\beta} \tag{5}$$

and

$$\mathcal{M}^{(j)}_{K^*} = g^2_{\pi K^* K} \epsilon_1^{\alpha} \epsilon_2^{\beta} \frac{1}{t - m_K^2} (p_1 - 2p_3)_{\alpha} (p_2 - 2p_4)_{\beta},$$
$$\mathcal{M}^{(k)}_{K^*} = g^2_{\pi K^* K} \epsilon_1^{\alpha} \epsilon_2^{\beta} \frac{1}{u - m_K^2} (p_1 - 2p_4)_{\alpha} (p_2 - 2p_3)_{\beta}, \tag{6}$$
$$\mathcal{M}^{(l)}_{K^*} = -g_{\pi\pi K^* K^*} \epsilon_1^{\alpha} \epsilon_2^{\beta} g_{\alpha\beta},$$

respectively. Finally, the amplitudes for $K^* \bar{K}^* \to \rho\rho$ are

$$\mathcal{M}^{(m)}_{K^*} = g^2_{\rho K^* K^*} \epsilon_1^{\alpha} \epsilon_3^{*\beta} \epsilon_2^{\gamma} \epsilon_4^{*\delta} \frac{1}{t - m^2_{K^*} + i m_{K^*} \Gamma_{K^*}} \left[-g^{\mu\nu} + \frac{(p_1 - p_3)^{\mu} (p_1 - p_3)^{\nu}}{m^2_{K^*}} \right]$$
$$\times [(2p_3 - p_1)_{\alpha} g_{\beta\mu} - (p_1 + p_3)_{\mu} g_{\alpha\beta} + (2p_1 - p_3)_{\beta} g_{\alpha\mu}][(p_2 + p_4)_{\gamma} g_{\delta\nu} + (p_2 - 2p_4)_{\nu} g_{\gamma\delta} + (p_4 - 2p_2)_{\delta} g_{\gamma\nu}],$$
$$\mathcal{M}^{(n)}_{K^*} = g^2_{\rho K^* K^*} \epsilon_1^{\alpha} \epsilon_4^{*\beta} \epsilon_2^{\gamma} \epsilon_3^{*\delta} \frac{1}{u - m^2_{K^*} + i m_{K^*} \Gamma_{K^*}} \left(-g^{\mu\nu} + \frac{(p_1 - p_4)^{\mu} (p_1 - p_4)^{\nu}}{m^2_{K^*}} \right)$$
$$\times [(2p_4 - p_1)_{\alpha} g_{\beta\mu} - (p_1 + p_4)_{\mu} g_{\alpha\beta} + (2p_1 - p_4)_{\beta} g_{\alpha\mu}][(p_2 + p_3)_{\gamma} g_{\delta\nu} + (p_2 - 2p_3)_{\nu} g_{\gamma\delta} + (p_3 - 2p_2)_{\delta} g_{\gamma\nu}],$$
$$\mathcal{M}^{(o)}_{K^*} = g_{\rho\rho K^* K^*} \epsilon_1^{\alpha} \epsilon_3^{*\beta} \epsilon_2^{\gamma} \epsilon_4^{*\delta} g_{\alpha\beta} g_{\gamma\delta} + g_{\rho\rho K^* K^*} \epsilon_1^{\alpha} \epsilon_3^{*\beta} \epsilon_2^{\gamma} \epsilon_4^{*\delta} g_{\alpha\delta} g_{\beta\gamma} + g_{\rho\rho K^* K^*} \epsilon_1^{\alpha} \epsilon_3^{*\beta} \epsilon_2^{\gamma} \epsilon_4^{*\delta} g_{\alpha\gamma} g_{\beta\delta}. \tag{7}$$

In the above equations, p_i denotes the momentum of particle i. We keep the convention that particles 1 and 2 stand for initial-state mesons, and particles 3 and 4 stand for final-state mesons on the left and right sides of the diagrams, respectively. The Mandelstam variables $s = (p_1 + p_2)^2$, $t = (p_1 - p_3)^2$, and $u = (p_1 - p_4)^2$ have also been used. We apply here the K^* meson propagator with its decay width, Γ_{K^*}, and use the isospin averaged value for the K^* meson decay width, $\Gamma_{K^*} = 49.1$ MeV [32].

In order to take the finite size of the hadron into consideration when evaluating amplitudes, we apply the following form factor at each interaction vertex for the u,t channel and the s channel, respectively:

$$F_{u,t}(\vec{q}) = \frac{\Lambda^2 - m^2_{\rm ex}}{\Lambda^2 + \vec{q}^2}, \quad F_s(\vec{q}) = \frac{\Lambda^2 + m^2_{\rm ex}}{\Lambda^2 + \omega^2}, \tag{8}$$

with $\vec{q}^2$ being the squared three-momentum transfer for t and u channels, and ω^2 being the total energy of the incoming particles for the s channel taken in the center-of-mass frame. $m_{\rm ex}$ is the mass of the exchanged particle in each diagram shown in Fig. 1. For the four point contact interaction we use the form factor of

$$F_c(\vec{k}) = \left(\frac{\Lambda^2}{\Lambda^2 + \vec{k}^2} \right)^2 \tag{9}$$

with $\vec{k}$ being the average value of the squared three-momenta used in the vertex form factors for the given channels at each process. We set the cutoff parameter Λ to be $\Lambda = 1.8$ GeV [33]. The final isospin- and spin-averaged cross section is given by

$$\sigma = \frac{1}{64\pi^2 s g_1 g_2} \frac{|\vec{p}_f|}{|\vec{p}_i|} \int d\Omega \overline{|\mathcal{M}|^2} F^4, \tag{10}$$

where g_1 and g_2 are the degeneracy factors of the initial 1 and 2 particles; $g_1 = (2I_1 + 1)(2S_1 + 1)$ and $g_2 = (2I_2 + 1)(2S_2 + 1)$, respectively. $\overline{|\mathcal{M}|^2}$ represents the squared amplitude of all processes in Eq. (2) obtained by summing over the isospins and spins of both the initial and final particles. $|\vec{p}_i|$ and $|\vec{p}_f|$ in Eq. (10) stand for the three-momenta of the initial and final particles in the center-of-mass frame.

Using the same method, we investigate hadronic effects on a K meson during the hadronic stage in heavy-ion collisions. We consider interactions of the K meson with π, ρ, K, and K^* mesons: $K\pi \to \rho K^*$, $K\rho \to \pi K^*$, $K\bar{K} \to \pi\pi$, $K\bar{K} \to \rho\rho$, and $K\bar{K}^* \to \pi\rho$. Among these, however, two processes, $K\pi \to \rho K^*$ and $K\rho \to \pi K^*$, are the same as the inverse processes of the K^* meson interacting with ρ mesons and pions as shown in Figs. 1(d)–1(f) and Figs. 1(a)–1(c), respectively, and the process $K\bar{K}^* \to \pi\rho$ is the same as that of the K^* meson interacting with $\bar{K}$ mesons, Figs. 1(g)–1(i). Therefore, all we need to consider more are the following amplitudes:

$$\mathcal{M}_{\bar{K}K \to \pi\pi} \equiv \mathcal{M}^{(a)}_K + \mathcal{M}^{(b)}_K,$$
$$\mathcal{M}_{\bar{K}K \to \rho\rho} \equiv \mathcal{M}^{(c)}_K + \mathcal{M}^{(d)}_K + \mathcal{M}^{(e)}_K, \tag{11}$$

for processes $K\bar{K} \to \pi\pi$ and $K\bar{K} \to \rho\rho$. We show the diagrams for these processes in Fig. 2.

In evaluating the amplitude for the process $K\bar{K} \to \pi\pi$ we have not considered a four point interaction term like the diagram shown in Fig. 2(e) for the $K\bar{K} \to \rho\rho$ process. It is known that the strength of the contact term at low energy is fixed in chiral perturbation theory. In an effective Lagrangian that includes the vector meson [37], one can find that the direct contact term for $K\bar{K} \to \pi\pi$ is smaller than that coming from the vector meson exchange. The magnitude of the vector meson exchange can be estimated by taking the static limit of the vector meson diagrams. One then finds that its form effectively becomes a four-point-type interaction and that its strength is a factor 3 larger than that coming from the direct contact term that we neglected. The detailed argument is given in the Appendix.

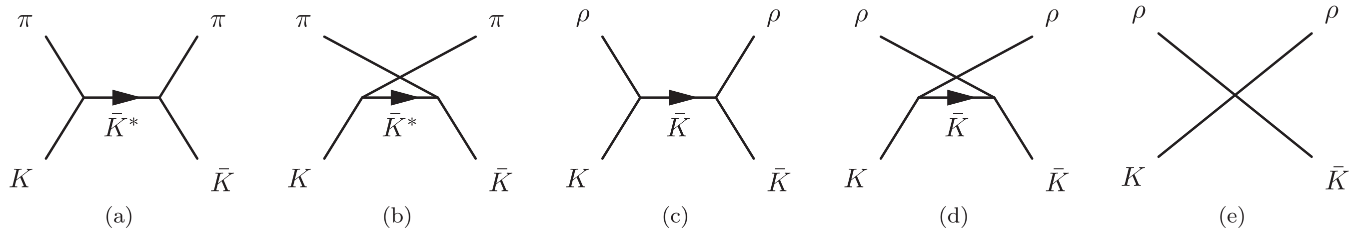

FIG. 2. Born diagrams for the K meson absorption by $\bar{K}$ mesons: (a, b) $K\bar{K} \to \pi\pi$ and (c–e) $K\bar{K} \to \rho\rho$.

The amplitudes for processes $K\bar{K} \to \pi\pi$ and $K\bar{K} \to \rho\rho$ are

$$\mathcal{M}_K^{(a)} = \frac{g_{\pi K^* K}^2}{t - m_{K^*}^2 + i m_{K^*}\Gamma_{K^*}}(p_1 + p_3)_\mu (p_2 + p_4)_\nu \times \left[-g^{\mu\nu} + \frac{(p_1 - p_3)^\mu (p_1 - p_3)^\nu}{m_{K^*}^2}\right],$$

$$\mathcal{M}_K^{(b)} = \frac{g_{\pi K^* K}^2}{u - m_{K^*}^2 + i m_{K^*}\Gamma_{K^*}}(p_1 + p_4)_\mu (p_2 + p_3)_\nu \times \left[-g^{\mu\nu} + \frac{(p_1 - p_4)^\mu (p_1 - p_4)^\nu}{m_{K^*}^2}\right] \tag{12}$$

and

$$\mathcal{M}_K^{(c)} = g_{\rho K K}^2 \epsilon_3^{*\alpha} \epsilon_4^{*\beta} \frac{1}{t - m_K^2}(2p_1 - p_3)_\alpha (2p_2 - p_4)_\beta,$$

$$\mathcal{M}_K^{(d)} = g_{\rho K K}^2 \epsilon_4^{*\alpha} \epsilon_3^{*\beta} \frac{1}{u - m_K^2}(2p_1 - p_4)_\alpha (2p_2 - p_3)_\beta,$$

$$\mathcal{M}_K^{(e)} = -g_{\rho\rho K K} \epsilon_3^{*\alpha} \epsilon_4^{*\beta} g_{\alpha\beta}, \tag{13}$$

respectively. Then, using Eqs. (8) and (10) we evaluate the K meson absorption cross sections.

Lastly we consider the possibility of the K^* meson formation from pions and kaons. The scattering cross section for the K^* meson production is given by the spin-averaged relativistic Breit-Wigner cross section:

$$\sigma_{K\pi \to K^*} = \frac{g_{K^*}}{g_K g_\pi} \frac{4\pi}{p_{\rm cm}^2} \frac{s\Gamma_{K^* \to K\pi}^2}{\left(m_{K^*}^2 - s\right)^2 + s\Gamma_{K^* \to K\pi}^2}, \tag{14}$$

with g_π, g_K, and g_{K^*} being the degeneracy of pions, kaons and K^* mesons, respectively, with $g_i = (2S_i + 1)(2I_i + 1)$ and $p_{\rm cm}$ the momentum in the center-of-mass frame. $\Gamma_{K^* \to K\pi}$ is the total decay width for a reaction $K\pi \to K^* \to K\pi$ as a function of $\sqrt{s}$. We take the following $\sqrt{s}$-dependent decay width $\Gamma_{K^* \to K\pi}$ of the K^* meson:

$$\Gamma_{K^* \to K\pi}(\sqrt{s}) = \frac{g_{\pi K^* K}^2}{2\pi s} p_{\rm cm}^3(\sqrt{s}). \tag{15}$$

It should be noted that through the rate equation to be discussed in the next section we effectively take into account the effect from the imaginary part in the self-energy of the K^* meson, which is not necessarily in equilibrium with the pion background at each instance. Hence, there might also be some changes in the real part of the K^* meson self-energy, or equivalently the K^* meson mass shift. However, the chiral order parameter at finite temperature is found to drop sharply only near the phase transition point. Therefore, we expect the change of the K^* meson mass to be important only near the phase transition point which influences the initial K^* numbers. In this paper, as we are interested in the relative change of the K^*/K ratio as a function of the system temperature and lifetime, which is mainly determined by the decay and production of K^* mesons during and dominantly at later stages of the hadronic evolution, we do not consider the explicit changes of the K^* meson mass caused by the real part of the K^* self-energy, though we consider such changes from the processes we have evaluated, which correspond to the effects from the imaginary part of the K^* meson self-energy.

We show in Fig. 3 the cross sections for the absorption of both the K^* meson and the K meson by π, ρ, K, and K^*

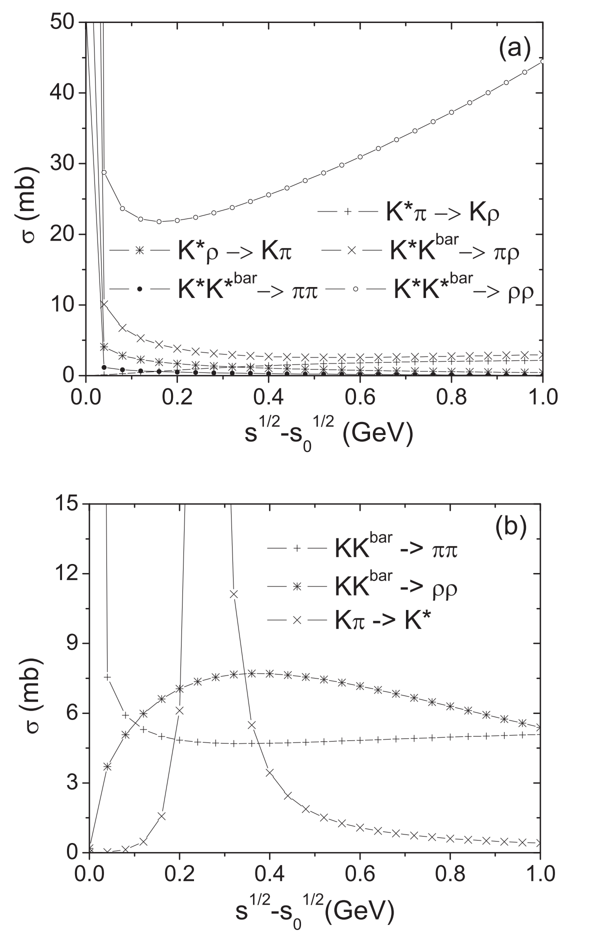

FIG. 3. Absorption cross sections for (a) the K^* meson by $\pi, \rho, K,$ and K^* mesons via processes $K^*\pi \to \rho K, K^*\rho \to \pi K$, $K^*\bar{K} \to \rho\pi$, $K^*\bar{K}^* \to \pi\pi$, and $K^*\bar{K}^* \to \rho\rho$, and those for (b) the K meson via processes $K\bar{K} \to \pi\pi$, $K\bar{K} \to \rho\rho$, and $K\pi \to K^*$.

mesons via processes shown in Figs. 1 and 2 as functions of the total center-of-mass energy $s^{1/2}$ above the threshold energy $s_0^{1/2}$ of each process. We see in Fig. 3 the general characteristics that cross sections have a peak near the threshold energy for the endothermic processes, e.g., $K^*\pi \to \rho K$ and $K\bar{K} \to \rho\rho$, while cross sections for the exothermic processes, e.g., $K^*\rho \to \pi K$, $K^*\bar{K} \to \rho\pi$, $K^*\bar{K}^* \to \pi\pi$, $K^*\bar{K}^* \to \rho\rho$, and $K\bar{K} \to \pi\pi$, become infinite near the threshold. We also see that contributions from the contact terms shown in Figs. 1(c), 1(f) 1(i), 1(l), 1(o), and 2(e) to amplitudes in all processes are significant.

We notice that the K^* meson is absorbed more easily by strange mesons, kaons and K^* mesons, than by light mesons, pions and ρ mesons; the absorption cross sections of the K^* meson by K^* mesons and kaons, $K^*\bar{K}^* \to \rho\rho$ and $K^*\bar{K} \to \rho\pi$, are larger than those by ρ mesons and pions, $K^*\rho \to \pi K$ and $K^*\pi \to \rho K$. We also see that the annihilation cross sections for both the K^* meson and K meson are larger when ρ mesons are produced than when pions are produced; the cross section for $K^*\bar{K}^* \to \rho\rho$ is larger than that for $K^*\bar{K}^* \to \pi\pi$, and the cross section for $K\bar{K} \to \rho\rho$ is also larger than that for $K\bar{K} \to \pi\pi$.

The cross section for $K^*\bar{K}^* \to \rho\rho$ is an order of magnitude larger than other processes, and seems to reflect the effect from two interaction mechanisms between three vector mesons. All particles participating in the process $K^*\bar{K}^* \to \rho\rho$ are vector mesons, and thus two $\mathcal{L}_{\rho K^* K^*}$ in Eq. (1) are needed to describe the process $K^*\bar{K}^* \to \rho\rho$. It has already been shown that the interaction between three vector mesons increases the absorption cross section in the effective Lagrangian approach [26].

It seems unusual that the cross section for $K^*\bar{K}^* \to \rho\rho$ rises with increasing energy even though the form factor has been correctly used to kill the artificial growth of the cross section with the energy. This behavior recalls the rise of the total cross section for $p\bar{p}$ collisions at high energy. It has been already well known that the resonance exchange is largely responsible for an increase of the cross section in high-energy scattering. In this paper the K^* meson exchange in the reaction $K^*\bar{K}^* \to \rho\rho$ causes the rise of the cross section even at relatively low energy less than 1 GeV. The introduction of the decay width in the propagator Γ_{K^*}, however, does not contribute to this behavior at all. Instead it merely reduces a little bit the amplitudes for the process having a K^* meson exchange. Finally, we also find that the cross section for the formation of the K^* meson from pions and K mesons, Eq. (14), is not small at all, compared to cross sections for other processes.

III. TIME EVOLUTIONS OF THE K^* AND K MESON ABUNDANCES

We consider the time evolutions of the abundance for both the K^* meson and kaon based on the cross sections evaluated in the previous section. We build a coupled evolution equation for both particles consisting of densities and abundances for mesons participating in all processes shown in Fig. 1; π, ρ, K, and K^* mesons:

$$\begin{aligned}
\frac{dN_{K^*}(\tau)}{d\tau} &= \langle\sigma_{K\rho\to K^*\pi}v_{K\rho}\rangle n_\rho(\tau)N_K(\tau) - \langle\sigma_{K^*\pi\to K\rho}v_{K^*\pi}\rangle n_\pi(\tau)N_{K^*}(\tau) + \langle\sigma_{K\pi\to K^*\rho}v_{K\pi}\rangle n_\pi(\tau)N_K(\tau)\\
&\quad - \langle\sigma_{K^*\rho\to K\pi}v_{K^*\rho}\rangle n_\rho(\tau)N_{K^*}(\tau) + \langle\sigma_{\rho\pi\to K^*\bar{K}}v_{\rho\pi}\rangle n_\pi(\tau)N_\rho(\tau) - \langle\sigma_{K^*\bar{K}\to\rho\pi}v_{K^*\bar{K}}\rangle n_K(\tau)N_{K^*}(\tau)\\
&\quad + \langle\sigma_{\pi\pi\to K^*\bar{K}^*}v_{\pi\pi}\rangle n_\pi(\tau)N_\pi(\tau) - \langle\sigma_{K^*\bar{K}^*\to\pi\pi}v_{K^*\bar{K}^*}\rangle n_{\bar{K}^*}(\tau)N_{K^*}(\tau) + \langle\sigma_{\rho\rho\to K^*\bar{K}^*}v_{\rho\rho}\rangle n_\rho(\tau)N_\rho(\tau)\\
&\quad - \langle\sigma_{K^*\bar{K}^*\to\rho\rho}v_{K^*\bar{K}^*}\rangle n_{\bar{K}^*}(\tau)N_{K^*}(\tau) + \langle\sigma_{\pi K\to K^*}v_{\pi K}\rangle n_\pi(\tau)N_K(\tau) - \langle\Gamma_{K^*}\rangle N_{K^*}(\tau),\\
\frac{dN_K(\tau)}{d\tau} &= \langle\sigma_{\pi\pi\to K\bar{K}}v_{\pi\pi}\rangle n_\pi(\tau)N_\pi(\tau) - \langle\sigma_{K\bar{K}\to\pi\pi}v_{K\bar{K}}\rangle n_{\bar{K}}(\tau)N_K(\tau) + \langle\sigma_{\rho\rho\to K\bar{K}}v_{\rho\rho}\rangle n_\rho(\tau)N_\rho(\tau)\\
&\quad - \langle\sigma_{K\bar{K}\to\rho\rho}v_{K\bar{K}}\rangle n_{\bar{K}}(\tau)N_K(\tau) + \langle\sigma_{K^*\pi\to K\rho}v_{K^*\pi}\rangle n_\pi(\tau)N_{K^*}(\tau) - \langle\sigma_{K\rho\to K^*\pi}v_{K\rho}\rangle n_\rho(\tau)N_K(\tau)\\
&\quad + \langle\sigma_{K^*\rho\to K\pi}v_{K^*\rho}\rangle n_\rho(\tau)N_{K^*}(\tau) - \langle\sigma_{K\pi\to K^*\rho}v_{K\pi}\rangle n_\pi(\tau)N_K(\tau) + \langle\sigma_{\rho\pi\to K^*\bar{K}}v_{\rho\pi}\rangle n_\pi(\tau)N_\rho(\tau)\\
&\quad - \langle\sigma_{K^*\bar{K}\to\rho\pi}v_{K^*\bar{K}}\rangle n_{\bar{K}}(\tau)N_{K^*}(\tau) + \langle\Gamma_{K^*}\rangle N_{K^*}(\tau) - \langle\sigma_{\pi K\to K^*}v_{\pi K}\rangle n_\pi(\tau)N_K(\tau),
\end{aligned} \tag{16}$$

where $n_i(\tau)$ is the density of a light meson i in the hadronic matter at proper time τ, and $N_j(\tau)$ is the abundance of the other light meson j in each process shown in Fig. 1 at proper time τ. $n_i(\tau)$ for pions and ρ mesons is evaluated from

$$\begin{aligned}
n_i(\tau) &= \frac{g_i}{2\pi^2}\int_0^\infty \frac{p^2dp}{e^{\sqrt{p^2+m_i^2}/T(\tau)}-1}\\
&\approx \frac{g_i}{2\pi^2}m_i^2T(\tau)K_2\left[\frac{m_i}{T(\tau)}\right],
\end{aligned} \tag{17}$$

by assuming that they are in thermal equilibrium, and varies in time through the temperature profile introduced below, Eq. (18). We obtain $N_j(\tau)$ by multiplying Eq. (17) by the hadronization volume $V(\tau)$. In Eq. (17), g_i is the degeneracy factor for a particle i and K_2 is the modified Bessel function of the second kind.

$n_i(\tau)$ and $N_j(\tau)$ are functions of the proper time through the temperature profile developed to describe the dynamics of relativistic heavy-ion collisions. We use the schematic model of a system with an accelerated transverse expansion based on the boost invariant Bjorken picture [29,38]:

$$\begin{aligned}
V(\tau) &= \pi[R_c + v_c(\tau-\tau_c) + a_c/2(\tau-\tau_c)^2]^2\tau c,\\
T(\tau) &= T_c - (T_h - T_f)\left(\frac{\tau-\tau_h}{\tau_f-\tau_h}\right)^{4/5},
\end{aligned} \tag{18}$$

with T_h and τ_f being the hadronization temperature and the freeze-out time, respectively. Equation (18) describes the system of the quark-gluon plasma expanding with its transverse

TABLE I. Values for the volume and temperature profiles in the schematic model Eq. (18).

	Temperature (MeV)	Time (fm/c)
$R_c = 8.0$ fm	$T_c = 175$	$\tau_c = 5.0$
$v_c = 0.4c$	$T_h = 175$	$\tau_h = 7.5$
$a_c = 0.02c^2/\text{fm}$	$T_f = 125$	$\tau_f = 17.3$

velocity v_c and transverse acceleration a_c starting from its final transverse size R_c at the chemical freeze-out time τ_c. The temperature of the system decreases from the hadronization temperature to the kinetic freeze-out temperature T_f. The values used in Eq. (18) are summarized in Table I.

In the rate equations, Eq. (16), $\langle\sigma_{ab\to cd}v_{ab}\rangle$ is the thermally averaged cross section for initial two particles in a two-body process $ab \to cd$ given by [39]

$$\begin{aligned}\langle\sigma_{ab\to cd}v_{ab}\rangle &= \frac{1}{1+\delta_{ab}}\frac{\int d^3\vec{p}_a d^3\vec{p}_b f_a(\vec{p}_a) f_b(\vec{p}_b)\sigma_{ab\to cd}v_{ab}}{\int d^3\vec{p}_a d^3\vec{p}_b f_a(\vec{p}_a) f_b(\vec{p}_b)} \\ &= \frac{1}{1+\delta_{ab}}\frac{T^4}{4m_a^2K_2(m_a/T)m_b^2K_2(m_b/T)} \\ &\quad\times\int_{z_0}^{\infty} dz K_1(z)\sigma(z^2T^2)[z^2-(m_a+m_b)^2/T^2] \\ &\quad\times[z^2-(m_a-m_b)^2/T^2], \end{aligned} \tag{19}$$

with $z_0 = \max((m_a+m_b)/T,(m_c+m_d)/T)$, K_1 and K_2 being the modified Bessel function of the second kind, f_i being the Boltzmann momentum distribution of the particle i, $f_i(\vec{p}) = e^{-\sqrt{\vec{p}^2+m_i^2}}$, respectively. v_{ab} is the relative velocity of interacting particles a and b, $v_{ab} = \sqrt{(p_a\cdot p_b)^2 - m_a^2m_b^2}/(E_aE_b)$. $\langle\Gamma_{K^*}\rangle$ in Eq. (16) is the thermally averaged decay width of K^* mesons, Eq. (15), $\langle\Gamma_{K^*}\rangle = \Gamma_{K^*}(m_{K^*})K_1(m_{K^*}/T)/K_2(m_{K^*}/T)$, which has been obtained in the same methods as used in Eq. (19).

The K^* meson abundance at τ, N_{K^*}, depends not only on the dissociation reactions like $K^*\pi \to \rho K$, $K^*\rho \to \pi K$, $K^*\bar{K} \to \rho\pi$, $K^*\bar{K}^* \to \pi\pi$, and $K^*\bar{K}^* \to \rho\rho$ but also on the production reactions, or the inverse reactions of the dissociation reactions, such as $\rho K \to K^*\pi$, $\pi K \to K^*\rho$, $\rho\pi \to K^*\bar{K}$, $\pi\pi \to K^*\bar{K}^*$, and $\rho\rho \to K^*\bar{K}^*$. We have taken both reactions into consideration in building the coupled equation for both the K^* meson and kaon in Eq. (16). We have used the detailed balance relation when evaluating thermally averaged cross sections of the inverse reactions from the results for forward processes shown in Fig. 3. The results are shown in Fig. 4.

As we see in Fig. 4, thermally averaged cross sections of the dissociation reactions are bigger than those of the production reactions for the exothermic reactions. In the case of the endothermic reaction like $K^*\pi \to \rho K$, the thermalized production cross section is bigger than that for the dissociation

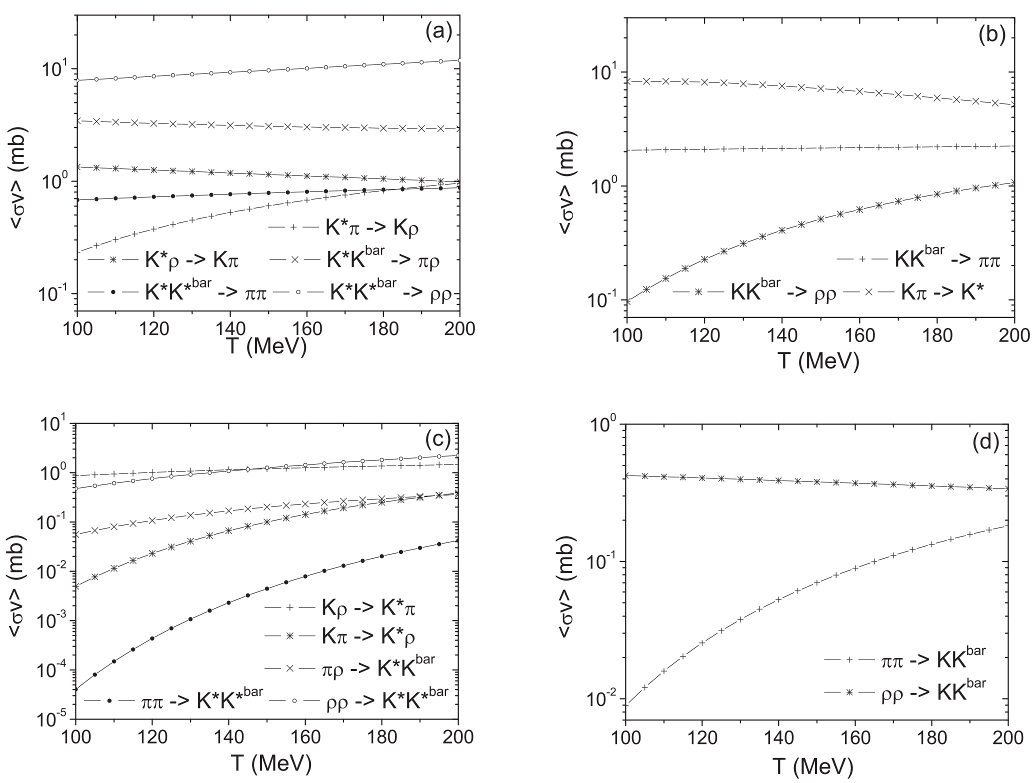

FIG. 4. Thermally averaged cross sections for the absorption of (a) a K^* meson by π, ρ, K, and K^* mesons via processes $K^*\pi \to \rho K$, $K^*\rho \to \pi K$, $K^*\bar{K} \to \rho\pi$, $K^*\bar{K}^* \to \pi\pi$, and $K^*\bar{K}^* \to \rho\rho$, and those for (b) a K meson via processes $K\bar{K} \to \pi\pi$, $K\bar{K} \to \rho\rho$, and $K\pi \to K^*$. Thermally averaged cross sections for their inverse processes (c) $\rho K \to K^*\pi$, $\pi K \to K^*\rho$, $\rho\pi \to K^*\bar{K}$, $\pi\pi \to K^*\bar{K}^*$, and $\rho\rho \to K^*\bar{K}^*$ for a K^* meson and (d) $\pi\pi \to K\bar{K}$ and $\rho\rho \to K\bar{K}$ for a K meson.

reaction. Both thermalized cross sections are comparable for the other endothermic reaction, $K\bar{K} \to \rho\rho$.

In general, the smaller the threshold energy, mass, and degeneracy, the bigger the thermally averaged cross section in the two-body process. We find that the thermally averaged cross section for K^* formation, $K\pi \to K^*$, becomes more significant than those for other reactions. However, the unusually rising cross section in energy for the reaction $K^*\bar{K}^* \to \rho\rho$ has been suppressed in the thermalized medium as shown in Fig. 4(a).

When solving the coupled differential equation for both the K^* meson and kaon abundances, we have treated abundances of their antiparticles $\bar{K}^*$ and $\bar{K}$ mesons also as variables using the strangeness chemical potential μ_s, i.e., $N_{\bar{K}^*} = e^{-2\mu_s/T(\tau)}N_{K^*}$ and the same for antikaons. In other words, we have not considered that K^* mesons and kaons are in thermal equilibrium during the expansion of the hadronic matter, while we calculate the thermally averaged cross section Eq. (19) using the thermal distributions of hadrons involved. However, the initial yield of kaons at chemical freeze-out has been evaluated to be 88.1 using the statistical hadronization model, Eq. (17) with the strangeness chemical potential $\mu_s = 10$ MeV and the hadronization volume $V_H = 1908$ fm^3 [30], whereas the initial yield of K^* mesons has been obtained from

$$N_{K^*}(\tau) = V_H \frac{g_{K^*}}{2\pi^2}\int_{m_{\rm th}}^{\infty}\frac{dm}{N_{\rm BW}}\frac{\Gamma_{K^*}}{(m-m_{K^*})^2+\Gamma_{K^*}^2/4} \times \int_0^{\infty}\frac{p^2dp}{e^{(\sqrt{p^2+m^2}-\mu_s)/T(\tau)}-1}, \quad (20)$$

to take the width of the K^* meson into consideration. In Eq. (20), $m_{\rm th}$ is the threshold energy for the $K^* \to K\pi$ decay channel and $N_{\rm BW}$ is the normalization constant for the Breit-Wigner distribution. We obtain the K^* meson initial yield to be 55.7, which is slightly larger than 52.4 obtained without including the K^* meson width calculated with the formula given in Eq. (17).

In Fig. 5, we show the abundances of the K^* meson and kaon as a function of the proper time during the hadronic

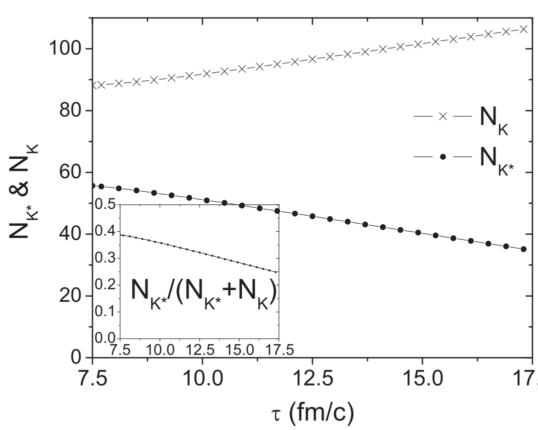

FIG. 5. Time evolution of the K^* meson and kaon abundances during the hadronic stage in central Au+Au collisions at $\sqrt{s_{NN}} = 200$ GeV. The ratio of the K^* meson abundance to the sum of the K^* meson and kaon abundances is shown in the inset.

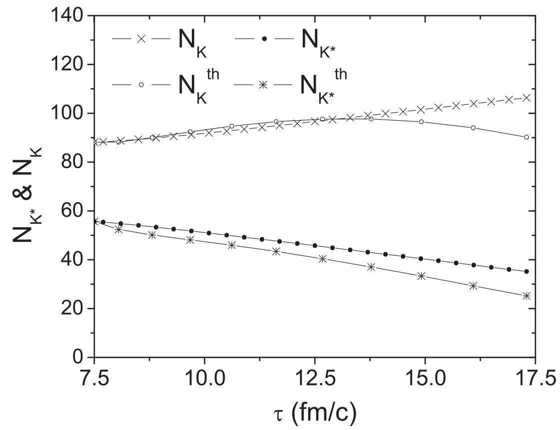

FIG. 6. A comparison between the K^* meson and kaon abundances due to all hadronic interactions shown in Figs. 1 and 2 and those from the thermal model prediction at each time and temperature.

stage of heavy-ion collisions at $\sqrt{s_{NN}} = 200$ GeV. As we have expected, the K^* meson abundance decreases due to both interactions of K^* mesons with other hadrons and the decay of the K^* meson to the pion and kaon, eventually becoming 35.2 at 9.8 fm/c after the chemical freeze-out. On the other hand the abundance of the kaon increases up to 106.4 at the end of hadronic expansion. We find that throughout the time evolution the sum of the K^* meson and kaon abundances changes slightly from 143.8 to 141.5. We also show in the inset of Fig. 5 the variation of the ratio of the K^* meson abundance to the sum of the K^* meson and kaon abundances. The ratio decreases from the initial ratio from the statistical hadronization model 0.39 to 0.25 in the end.

Based on the analysis we find that about 37% of K^* mesons produced at chemical freeze-out disappear during the hadronic stage in heavy-ion collisions, making the invariant mass reconstruction of the total K^* meson difficult. We further find that the hadronic interactions shown in both Figs. 1 and 2 explain about 5% of the K^* meson loss, and the K^* meson decay, Eq. (15), and its formation, Eq. (14), are largely responsible for the K^* meson reduction in the hadronic medium. Our result is comparable to the 30% reduction of the previous statistical model prediction 0.33 ± 0.01 [10] to the experimental measurements 0.23 ± 0.05 [13].

We also consider the possibility of both the K^* meson and kaon thermalization during the hadronic expansion. Assuming that both mesons are in thermal equilibrium with the hadronic medium we evaluate the K^* meson and kaon abundances in time using Eqs. (17), (20), and (18), and show the results represented by $N_K^{\rm th}$ and $N_{K^*}^{\rm th}$ in Fig. 6.

As we see, $N_{K^*}^{\rm th}$ keeps decreasing all the time. However, $N_K^{\rm th}$ increases at the beginning of the hadronic stage, and finally decreases. This is due to the competition between the volume expansion and the decreasing rate caused by the thermal effects in Eq. (17), through the factor $m_K/T(\tau)$ inside the modified Bessel function of the second kind, implying that $N_K^{\rm th}$ and $N_{K^*}^{\rm th}$ depend on the size and also on the lifetime of the expanding fireball, Eq. (18). Nevertheless, one should note that the volume of the system expands in time with the total entropy almost preserved [40]. We find that abundances of most hadrons decrease during the hadronic expansion in the statistical hadronization model but that of the pion, the lightest hadron, increases in time to compensate the loss of entropy from heavier hadrons. We argue that the same mechanism is happening to strangeness hadrons for some time during the hadronic expansion. However, the ratio $N_{K^*}^{\rm th}/(N_K^{\rm th}+N_{K^*}^{\rm th})$ is not affected by the volume, and it keeps decreasing from 0.39 to 0.25 at the kinetic freeze-out.

We notice that recent measurements of the K^* meson yield in Pb+Pb collisions at $\sqrt{s_{NN}}=2.76$ TeV at the LHC provide 0.19 ± 0.05 [23] as the K^{*0}/K^- ratio. This value is also smaller than the statistical hadronization model prediction 0.30 evaluated with the hadronization temperature 156 MeV [41] at the LHC energy. The measurements indicate that more K^* mesons are lost during the hadronic expansion at LHC, leading to 37% reduction of the ratio.

IV. THE ABUNDANCE RATIO OF K^* MESONS TO KAONS IN HEAVY-ION COLLISIONS

Since the interactions of K^* mesons and kaons with light mesons considered in Figs. 1 and 2 take place during the hadronic stage at both BNL's Relativistic Heavy Ion Collider (RHIC) and LHC, it is necessary to understand general features of the variation of the K^* meson abundance in heavy-ion collisions. In order to analyze the reduction of the K^* meson in the hadronic medium we simplify the coupled equation, Eq. (16), by keeping the linear terms in N_K and N_{K^*} only:

$$\frac{dN_{K^*}(\tau)}{d\tau}=\gamma_K N_K(\tau)-\gamma_{K^*}N_{K^*}(\tau),$$
$$\frac{dN_K(\tau)}{d\tau}=-\gamma_K N_K(\tau)+\gamma_{K^*}N_{K^*}(\tau), \tag{21}$$

with

$$\gamma_{K^*}=\langle\sigma_{K^*\rho\to K\pi}v_{K^*\rho}\rangle n_\rho+\langle\sigma_{K^*\pi\to K\rho}v_{K^*\pi}\rangle n_\pi+\langle\Gamma_{K^*}\rangle,$$
$$\gamma_K=\langle\sigma_{K\pi\to K^*\rho}v_{K\pi}\rangle n_\pi+\langle\sigma_{K\rho\to K^*\pi}v_{K\rho}\rangle n_\rho+\langle\sigma_{K\pi\to K^*}v_{K\pi}\rangle n_\pi. \tag{22}$$

When the thermal cross sections and densities of light mesons are independent of time, the following analytic solutions are obtained from the coupled equation, Eq. (21):

$$N_{K^*}(\tau)=\frac{\gamma_K}{\gamma}N^0+\left(N_{K^*}^0-\frac{\gamma_K}{\gamma}N^0\right)e^{-\gamma(\tau-\tau_h)},$$
$$N_K(\tau)=\frac{\gamma_{K^*}}{\gamma}N^0+\left(N_K^0-\frac{\gamma_{K^*}}{\gamma}N^0\right)e^{-\gamma(\tau-\tau_h)}, \tag{23}$$

where the initial yields for both hadrons, N_K^0 and $N_{K^*}^0$, have been assumed, and N^0 is the sum of the K^* meson and kaon yields, $N^0=N_K^0+N_{K^*}^0$, at chemical freeze-out. The γ in Eq. (23) is the sum of the K^* meson and kaon widths in the hadronic phase, $\gamma=\gamma_K+\gamma_{K^*}$; γ_{K^*} and γ_K play roles of the collisional broadening of the width of the K^* meson and kaon in the hadronic medium, respectively.

In Eq. (23) time-independent terms represent abundances when time goes to infinity, and the sum of two solutions is preserved as its initial value $N_K^0+N_{K^*}^0$. As time goes on N_K increases while N_{K^*} decreases, and the rate at which the final number is reached in Eq. (23) is determined by the γ which takes into account hadronic interactions of K^* mesons and kaons with light mesons. If the γ is large, the abundance can change significantly for a short time.

Let us now investigate the time evolution of yield ratio of K^* mesons to kaons from the analytic solution of Eq. (23), $R(\tau)=N_{K^*}(\tau)/[N_K^*(\tau)+N_K(\tau)]$:

$$R(\tau)=\frac{N_{K^*}(\tau)}{N_{K^*}(\tau)+N_K(\tau)}=\frac{N_{K^*}(\tau)}{N^0}$$
$$=\frac{\gamma_K}{\gamma}+\left(\frac{N_{K^*}^0}{N^0}-\frac{\gamma_K}{\gamma}\right)e^{-\gamma(\tau-\tau_h)}. \tag{24}$$

We notice that $R(\tau)$ is also composed of two parts: a time-independent part and a transient part. After a long time τ the time-independent part $R(\infty)=\gamma_K/\gamma$ is expected to represent the K^* meson to the kaon ratio. How fast the abundance ratio approaches the time-independent part relies on γ, the sum of the K^* meson and kaon widths in the exponential function.

With these in mind let us investigate the variation in the abundance of K^* mesons and kaons obtained from Eq. (16). Since all thermally averaged cross sections and densities of the light mesons in γ_K and γ_{K^*} are functions of a time, solutions of Eq. (16) are different from the analytic solution of the simplified equation, Eq. (21). Nevertheless, we find that the solution of Eq. (16) keeps the same important characteristics of the analytic solutions from Eq. (21).

We first show in Fig. 7(a) γ obtained in Eq. (16) as a function of time. The γ decreases in time from 0.33 to 0.26 c/fm as the system cools down from 175 MeV at τ_H to 125 MeV at τ_f, reflecting that interactions between hadrons become less vigorous as the temperature of the system decreases. The γ_K or $\langle\sigma_{K\pi\to K^*\rho}v_{K\pi}\rangle n_\pi+\langle\sigma_{K\rho\to K^*\pi}v_{K\rho}\rangle n_\rho+\langle\sigma_{K\pi\to K^*}v_{K\pi}\rangle n_\pi$ in Eq. (22) decreases as the temperature decreases, but γ_{K^*} is almost constant during the hadronic stage; with decreasing temperature of the system, the part of γ_{K^*} or $\langle\sigma_{K^*\rho\to K\pi}v_{K^*\rho}\rangle n_\rho+\langle\sigma_{K^*\pi\to K\rho}v_{K^*\pi}\rangle n_\pi$ decreases whereas the thermal width of the K^* meson $\langle\Gamma_{K^*}\rangle$ slightly increases due to the factor $K_1(m_{K^*}/T)/K_2(m_{K^*}/T)$, meaning that K^* mesons live shorter at lower temperature.

We compare in Fig. 7(b) the abundance ratio variation $N_{K^*}/(N_K+N_{K^*})$ evaluated numerically from Eq. (16) for RHIC to γ_K/γ obtained from Eq. (24) at each time and temperature. γ_K/γ represents the expected hadronic interaction width ratio between kaons and K^* mesons plus kaons at each temperature and time. We anticipate that the abundance ratio of K^* mesons and kaons in Fig. 7 approaches to γ_K/γ as time goes on, like the ratio between those mesons obtained from the simplified rate equation, Eq. (24). We show in the inset of Fig. 7(b) how $\gamma(\tau-\tau_h)$ varies in time at RHIC. As we see, $\gamma(\tau-\tau_h)$ increases up to 2.5 for 9.8 fm/c. We expect that the similar term with $e^{-\gamma(\tau-\tau_h)}$ in the real solution suppresses the contribution of the time-dependent term as time goes on. The discrepancy between the abundance ratio and the γ_K/γ in Fig. 7(b) is attributable to both the contribution from nonlinear terms included in Eq. (16)—such as $K^*\bar{K}\to\rho\pi$, [Figs. 1(g)–1(i)], $K^*\bar{K}^*\to\pi\pi$, [Figs. 1(j)–1(l)], $K^*\bar{K}^*\to\rho\rho$ [Figs. 1(m)–1(o)], $K\bar{K}\to\pi\pi$ [Figs. 2(a)–2(b)], and $K\bar{K}\to\rho\rho$ [Figs. 2(c)–2(e)]—and the time delay

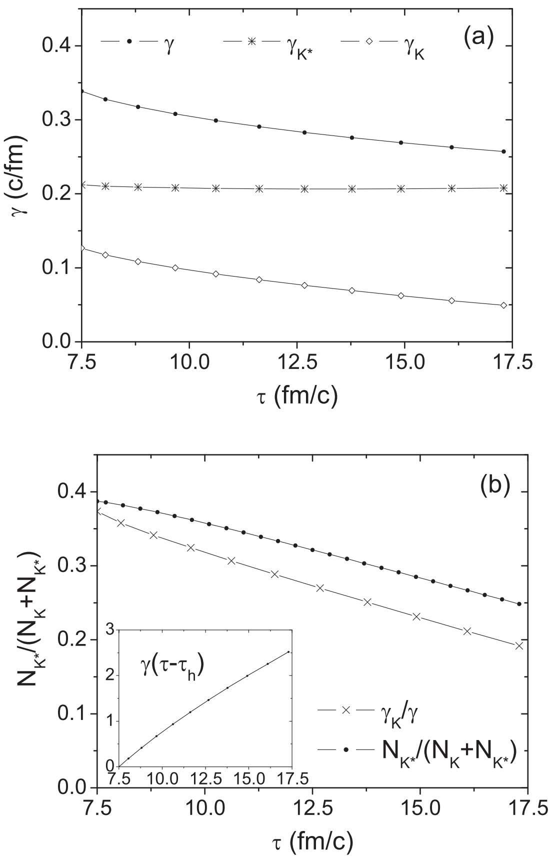

FIG. 7. (a) Variations of γ_K, γ_{K^*}, and $\gamma = \gamma_K + \gamma_{K^*}$ in time during the hadronic stage. (b) A comparison of the abundance ratio variation $N_{K^*}/(N_K + N_{K^*})$ obtained numerically from Eq. (16) for RHIC and $R(\tau = \infty) = \gamma_K/\gamma$ from Eq. (24) evaluated at each time and temperature. We show in the inset how $\gamma(\tau - \tau_h)$ changes in time.

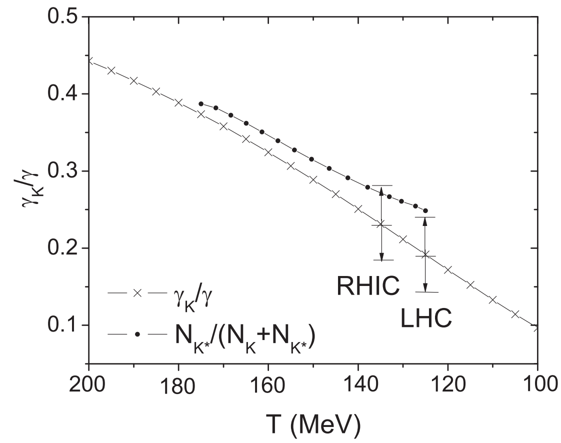

FIG. 8. Variations of γ_K/γ and $N_{K^*}/(N_K + N_{K^*})$ from Eq. (16) in temperature during the hadronic stage. We show measurements of the abundance ratio between K^* mesons and kaons, $N_{K^*}/(N_K + N_{K^*})$ 0.23 ± 0.05 at RHIC [13] and 0.19 ± 0.05 at LHC [23].

required to reach thermal equilibrium from the interactions of K^* mesons with light mesons in the hadronic medium.

Based on the above analysis we argue that the final ratio of the yield between K^* mesons and kaons in heavy-ion collisions is largely dependent on their interactions with other hadrons in the hadronic medium, γ_K and γ_{K^*}. Since $\gamma(\tau - \tau_h)$ keeps increasing during the hadronic stage, the transient term with $e^{-\gamma(\tau-\tau_h)}$ in the yield ratio $R(\tau)$ plays a negligible role at a later time during the hadronic interaction stage. Therefore, we see that the relative interaction ratio γ_K/γ mainly determines the final yield ratio between K^* mesons and kaons at the end of the hadronic stage.

We show in Fig. 8 γ_K/γ and $N_{K^*}/(N_K + N_{K^*})$ obtained from Eq. (16) as functions of the temperature of the system. We also show in Fig. 8 measurements of the abundance ratio between K^* mesons and kaons, $N_{K^*}/(N_K + N_{K^*})$, 0.23 ± 0.05 at RHIC [13], and 0.19 ± 0.05 at LHC [23]. We notice from Fig. 8 that the ratio of the K^* meson and kaon in heavy-ion collisions seems to reflect the interaction ratio between strange and light mesons, γ_K/γ, at the kinetic freeze-out temperature. We infer that the lower ratio $N_{K^*}/(N_K + N_{K^*})$ at LHC compared to that at RHIC is due to a lower kinetic freeze-out temperature at LHC than at RHIC.

It has been argued that the degree of the reduction of K^* meson yield during the hadronic stage in heavy-ion collisions is attributable to a lifetime of the hadronic stage. Since the system of quark-gluon plasma at LHC is much larger than that at RHIC, it has been assumed that the lifespan of the hadronic stage at LHC is also longer compared to that at RHIC, and thereby more K^* mesons are lost in the hadronic medium at LHC.

We find, however, from the investigation of the variation in the yield ratio between K^* mesons and kaons based on the solution of the rate equation, that the reduction of the K^* meson in heavy-ion collisions reflects the interaction of K^* mesons and kaons with light mesons at kinetic freeze-out. We argue that the degree of the K^* meson abundance reduction in heavy-ion collisions, or the reduction of the yield ratio between the K^* meson and kaon, is largely attributable to *the kinetic freeze-out temperature* via the interaction of K^* mesons and kaons with light mesons in the hadronic medium. The long lifespan of the hadronic stage just suppresses more a transient term, such as the second term in Eq. (24), contributing little to the change of the K^* meson to kaon ratio.

Due to both the larger number of particles and the larger volume of the system at LHC than at RHIC, the temperature is expected to drop more at LHC than at RHIC between the chemical freeze-out and kinetic freeze-out. Moreover, as has already been analyzed in the statistical hadronization model, the chemical freeze-out temperature at LHC, 156 MeV [41], is lower than that at RHIC, 162 MeV [42]. Therefore, it is natural that the kinetic freeze-out temperature at LHC is lower than that at RHIC, which can support the smaller abundance ratio between K^* mesons and kaons $N_{K^*}/(N_K + N_{K^*})$, 0.19 ± 0.05 at LHC compared with 0.23 ± 0.05 at RHIC.

The argument on the lower kinetic freeze-out temperature at LHC compared to that at RHIC, based on the investigation on the reduction of the K^* meson abundance at both RHIC and LHC, agrees with the recent UrQMD model study on the centrality dependence of resonance production in heavy-ion collisions [20]. The longest hadronic phase is expected for the largest system size available at the most central collisions, which leads to the lower kinetic freeze-out temperature with increasing centralities.

As has been already mentioned, how fast meson abundances change in the hadronic medium is governed by the sum of all the interactions involved, i.e., the width γ in Eq. (23). Therefore, in addition to the hadronic interactions considered in Figs. 1 and 2 all other interactions with various hadrons, i.e., nucleons, have to be taken into account to thoroughly understand the reduction of K^* mesons in heavy-ion collisions. Moreover, we also have to include more the feed down effects from heavier strangeness hadrons to fully consider the abundance ratio of the K^* meson to the kaon, which is left for future work.

V. CONCLUSION

We have studied the reduction of K^* mesons in heavy-ion collisions. We have focused on the hadronic effects on the K^* meson and kaon abundances during the hadronic stage of the cental Au+Au collisions at $\sqrt{s_{NN}} = 200$ GeV in order to understand the K^* meson yield difference between the experimental measurement and the statistical hadronization model prediction. We have evaluated absorption cross sections for both kaons and K^* mesons by π, ρ, K, and K^* mesons inside the hadronic medium. In describing the interaction between K^* mesons and kaons and light mesons, we have introduced one meson exchange model with the effective Lagrangian. Furthermore, we have built the coupled differential equation for K^* mesons and kaons, and have solved it to investigate the time evolution of the K^* meson and kaon abundances during the expansion of the hadronic matter.

We have found that the K^* meson and kaon abundances during the hadronic stage of heavy-ion collisions are dependent on absorption cross sections and their thermal average. We have shown that the sum of K^* and kaon abundances is almost preserved during the expansion, and the interaction of K^* mesons with light mesons controls the reduction or production of K^* mesons and kaons in the hadronic matter. Our analysis indicates that 37% of the total K^* mesons produced at the chemical freeze-out are lost during the hadronic expansion in the central Au+Au collisions at $\sqrt{s_{NN}} = 200$ GeV. We have found that among 37% about 5% of the total K^* mesons are converted into light mesons by hadronic interactions, and the remaining 32% reduction is due to the decay of K^* mesons to kaons and pions. We see that the loss of the K^* meson abundance in the hadronic medium explains very well the discrepancy of the K/K^* ratio between the statistical hadronization [10] model prediction and the experimental measurements [13].

We have shown that the results obtained here can be applied to the analysis of the K^* meson production at the LHC. We have found that all the interactions involved at RHIC must be present at LHC, and therefore widths γ_{K^*} and γ_K evaluated at the RHIC energy can be applied to the case at the LHC energy. Moreover, we have realized that the smaller ratio of K^*/K measured at the LHC energy indicates a lower temperature of the kinetic freeze-out at LHC compared to that at RHIC. We have shown that the yield ratio between K^* mesons and kaons is not mainly dependent on the lifetime of the hadronic stage in heavy-ion collisions, and the hadronic interaction width ratio of strange mesons with light mesons, γ_K/γ, determines the final yield ratio between K^* mesons and kaons. We therefore conclude that studying the yield of the K^* meson and its variation during the hadronic stage in relativistic heavy-ion collisions provides a chance to understand not only the production of K^* mesons but also the evolution of the hadronic medium in heavy-ion collisions.

ACKNOWLEDGMENTS

S.C. was supported by a 2015 Research Grant from Kangwon National University and a National Research Foundation of Korea (NRF) grant funded by the Korea government (MSIP) (No. 2016R1C1B1016270). S.H.L. was supported by the Korean ministry of education under the Grant No. 2016R1D1A1B03930089.

APPENDIX: FOUR POINT CONTACT TERM

We introduce the effective Lagrangian in the hidden gauge approach [37]. This approach has the advantage over the massive Yang-Mills approach in that chiral symmetry can be kept intact after introducing the vector meson without additionally introducing the axial vector meson [43,44]:

$$\begin{aligned}\mathcal{L} &= \mathcal{L}_A + a\mathcal{L}_V,\\ \mathcal{L}_V &= f_\pi^2 \mathrm{tr}\left[V_\mu - \frac{1}{2i}(D_\mu\xi_L\cdot\xi_L^\dagger + D_\mu\xi_R\cdot\xi_R^\dagger)\right]^2,\\ \mathcal{L}_A &= f_\pi^2 \mathrm{tr}\left[\frac{1}{2i}(D_\mu\xi_L\cdot\xi_L^\dagger - D_\mu\xi_R\cdot\xi_R^\dagger)\right]^2,\end{aligned} \tag{A1}$$

where a is taken to be 2 [43]. In the unitary gauge,

$$\xi = \xi_L^\dagger = \xi_R = e^{iP(x)\cdot\tau}, \tag{A2}$$

where $P(x)$ is taken to be the pseudoscalar octet field divided by the decay constant f_π. Then, to lowest order, we have

$$\begin{aligned}&\frac{1}{2i}(D_\mu\xi_L\cdot\xi_L^\dagger + D_\mu\xi_R\cdot\xi_R^\dagger)\\ &= \frac{1}{2i}[(\partial_\mu P)P - P\partial_\mu P],\\ &\frac{1}{2i}(D_\mu\xi_L\cdot\xi_L^\dagger - D_\mu\xi_R\cdot\xi_R^\dagger)\\ &= \left[-\partial_\mu P + \frac{1}{6}(\partial_\mu P)P^2 - \frac{2}{6}P(\partial_\mu P)P + \frac{1}{6}P^2\partial_\mu P\right].\end{aligned} \tag{A3}$$

Therefore, to lowest order

$$\begin{aligned}2\mathcal{L}_V &= 2f_\pi^2\mathrm{tr}\left\{V_\mu^2 - 2V_\mu\frac{1}{2i}[(\partial_\mu P)P - P\partial_\mu P]\right.\\ &\qquad\left. - \frac{1}{4}[(\partial_\mu P)P - P\partial_\mu P]^2\right\},\end{aligned} \tag{A4}$$

$$\mathcal{L}_A = f_\pi^2\mathrm{tr}\left\{(\partial_\mu P)^2 + \tfrac{1}{3}[(\partial_\mu P)P - P\partial_\mu P]^2\right\}. \tag{A5}$$

If the vector field V_μ is integrated out, Eq. (A4) vanishes and one is left with Eq. (A5), which corresponds to the lowest-order chiral Lagrangian. If the kinetic term for the vector meson is added so that the vector field becomes dynamical, the vector meson pseudoscalar coupling is obtained from $\mathcal{L}_V$ and one is left with the following four point contact term:

$$2\mathcal{L}_V + \mathcal{L}_A = f_\pi^2 \mathrm{tr}\left\{-\tfrac{1}{6}[(\partial_\mu P)P - P\partial_\mu P]^2\right\}. \tag{A6}$$

Now, consider $K + \bar{K} \to \pi + \pi$. The process can occur through the contact interaction given in Eq. (A6), or the vector meson exchange obtained by using the $V_\mu PP$ vertex in Eq. (A4) twice. Note that the mass term for the vector meson can be obtained by substituting $V_\mu = g\rho_\mu$ in Eq. (A4), which gives $m_V^2 = 2g^2 f_\pi^2$. In the static limit of the vector meson, the vector meson mass cancels the two factors of g and the extra f_π^2 appearing in the contracted vertex and hence leads to an effective vertex without the mass term given as follows:

$$\mathcal{L}_{\text{Vector-exchange}} = 2f_\pi^2 \mathrm{tr}\left\{\tfrac{1}{4}[(\partial_\mu P)P - P\partial_\mu P]^2\right\}. \tag{A7}$$

Comparing Eq. (A7) with Eq. (A6), we note that the contribution from the vector meson exchange diagram in the static vector meson limit is a factor 3 larger than that from the direct contact term. Hence, we neglect the direct contact term for the process $K + \bar{K} \to \pi + \pi$ in this paper.

[1] I. Arsene *et al.* (BRAHMS Collaboration), Nucl. Phys. A **757**, 1 (2005).
[2] B. B. Back *et al.* (PHOBOS Collaboration), Nucl. Phys. A **757**, 28 (2005).
[3] J. Adams *et al.* (STAR Collaboration), Nucl. Phys. A **757**, 102 (2005).
[4] K. Adcox *et al.* (PHENIX Collaboration), Nucl. Phys. A **757**, 184 (2005).
[5] M. Gyulassy and L. McLerran, Nucl. Phys. A **750**, 30 (2005).
[6] S. Gupta, X. Luo, B. Mohanty, H. G. Ritter, and N. Xu, Science **332**, 1525 (2011).
[7] P. Braun-Munzinger, J. Stachel, J. P. Wessels, and N. Xu, Phys. Lett. B **344**, 43 (1995).
[8] P. Braun-Munzinger, J. Stachel, J. P. Wessels, and N. Xu, Phys. Lett. B **365**, 1 (1996).
[9] P. Braun-Munzinger, I. Heppe, and J. Stachel, Phys. Lett. B **465**, 15 (1999).
[10] P. Braun-Munzinger, D. Magestro, K. Redlich, and J. Stachel, Phys. Lett. B **518**, 41 (2001).
[11] G. Torrieri and J. Rafelski, Phys. Lett. B **509**, 239 (2001).
[12] M. Bleicher and J. Aichelin, Phys. Lett. B **530**, 81 (2002).
[13] J. Adams *et al.* (STAR Collaboration), Phys. Rev. C **71**, 064902 (2005).
[14] M. M. Aggarwal *et al.* (STAR Collaboration), Phys. Rev. C **84**, 034909 (2011).
[15] G. Baym and H. Heiselberg, Phys. Lett. B **469**, 7 (1999).
[16] S. Jeon and V. Koch, Phys. Rev. Lett. **83**, 5435 (1999).
[17] J. Rafelski, J. Letessier, and G. Torrieri, Phys. Rev. C **64**, 054907 (2001).
[18] S. Vogel, J. Aichelin, and M. Bleicher, Phys. Rev. C **82**, 014907 (2010).
[19] G. Torrieri, R. Bellwied, C. Markert, and G. Westfall, J. Phys. G **37**, 094016 (2010).
[20] A. G. Knospe, C. Markert, K. Werner, J. Steinheimer and M. Bleicher, Phys. Rev. C **93**, 014911 (2016).
[21] S. A. Bass *et al.*, Prog. Part. Nucl. Phys. **41**, 255 (1998).
[22] M. Bleicher *et al.*, J. Phys. G **25**, 1859 (1999).
[23] B. B. Abelev *et al.* (ALICE Collaboration), Phys. Rev. C **91**, 024609 (2015).
[24] S. G. Matinyan and B. Muller, Phys. Rev. C **58**, 2994 (1998).
[25] K. L. Haglin, Phys. Rev. C **61**, 031902(R) (2000).
[26] Z. Lin and C. M. Ko, Phys. Rev. C **62**, 034903 (2000).
[27] Y. Oh, T. Song, and S. H. Lee, Phys. Rev. C **63**, 034901 (2001).
[28] L. Alvarez-Ruso and V. Koch, Phys. Rev. C **65**, 054901 (2002).
[29] L. W. Chen, C. M. Ko, W. Liu, and M. Nielsen, Phys. Rev. C **76**, 014906 (2007).
[30] S. Cho and S. H. Lee, Phys. Rev. C **88**, 054901 (2013).
[31] A. Martinez Torres, K. P. Khemchandani, F. S. Navarra, M. Nielsen, and L. M. Abreu, Phys. Rev. D **90**, 114023 (2014).
[32] J. Beringer *et al.* (Particle Data Group Collaboration), Phys. Rev. D **86**, 010001 (2012).
[33] G. E. Brown, C. M. Ko, Z. G. Wu, and L. H. Xia, Phys. Rev. C **43**, 1881 (1991).
[34] K. L. Haglin and C. Gale, Phys. Rev. C **63**, 065201 (2001).
[35] A. Martinez Torres, K. P. Khemchandani, L. M. Abreu, F. S. Navarra, and M. Nielsen, arXiv:1708.05784.
[36] L. M. Abreu, K. P. Khemchandani, A. Martnez Torres, F. S. Navarra and M. Nielsen, arXiv:1712.06019.
[37] M. Bando, T. Kugo, and K. Yamawaki, Phys. Rep. **164**, 217 (1988).
[38] L-W. Chen, V. Greco, C. M. Ko, S. H. Lee, and W. Liu, Phys. Lett. B **601**, 34 (2004).
[39] P. Koch, B. Muller, and J. Rafelski, Phys. Rep. **142**, 167 (1986).
[40] P. J. Siemens and J. I. Kapusta, Phys. Rev. Lett. **43**, 1486 (1979).
[41] J. Stachel, A. Andronic, P. Braun-Munzinger, and K. Redlich, J. Phys.: Conf. Ser. **509**, 012019 (2014).
[42] A. Andronic, P. Braun-Munzinger, K. Redlich, and J. Stachel, Nucl. Phys. A **904–905**, 535c (2013).
[43] U. G. Meissner, Phys. Rep. **161**, 213 (1988).
[44] S. H. Lee, C. Song, and H. Yabu, Phys. Lett. B **341**, 407 (1995).